33RD CONGRESS
OF THE INTERNATIONAL COUNCIL
OF THE AERONAUTICAL SCIENCES
STOCKHOLM, SWEDEN, 4-9 SEPTEMBER, 2022

ICAS 2022 SWEDEN

AN INVESTIGATION ON THE IMPROVEMENT FOR TANDEM WING PITCHING MOMENT CHARACTERISTICS

Xiangsheng Wang [1], Tielin Ma [2,3], Nanxuan Qiao [1], Jingcheng Fu [4]

[1] School of Aeronautic Science and Engineering, Beihang University, Beijing, PR China
[2] Institude of Unmanned System, Beihang University, Beijing, PR China
[3] Key Laboratory of Advanced Technology of Intelligent Unmanned Flight System, Ministry of Industry and Information Technology, Beijing, PR China
[4] School of Transportation Science and Engineering, Beihang University, Beijing, PR China

Abstract

Foldable unmanned aerial vehicles employing tandem wings can equip twice as much wing area as the traditional configuration with a similar folded length and magnitude of wing bending moment, which makes it preferred for tube-launched long-endurance UAVs. However, the tandem wing exists a defect of nonlinear pitching-moment caused by wing-wing interaction in some degree, which has been rarely studied. Our investigation concentrates on the flow phenomenon between the front and rear wing and aims to achieve some improvement on pitching moment characteristics. First, the analysis of the aerodynamic characteristic differences between the two airfoils and the three-dimension configuration is conducted, and the different consequences of flow interactions are discussed respectively. Following that, a verification simulation that enlarges the front wing span is conducted to reveal the different influences of downwash and wingtip vortex. Finally, two modified wingtip shapes are studied and verified to meet the wingspan constraints. The conclusion is the wingtip vortex of the front wing and the induced spanwise flow of the rear wing causes the poor pitching moment characteristic. The downwash of the front wing is a secondary effect. Declining the aerodynamic efficiency loss of the rear wing can relieve the pitching moment nonlinearity caused by a forward tendency of the aerodynamic center at a negative angle of attack. Optimizing the front wing wingtip shape improves the linearity of the pitching-moment, and a better rear wing aerodynamic performance is accompanied. This article provides a reference to the wingtip design and aerodynamic optimization of the tandem wing.

Keywords: UAV, Tandem wing, Aerodynamic characteristic, Longitudinal characteristic, Wingtips.

1. Introduction

Unmanned aerial vehicle (UAV) systems have been broadly applied across the globe in recent years [1]. A foldable wing is a common requirement that can realize launching from a tubular catapult while having enough wings area in the flight [2]. The tandem wing configuration can deploy a larger wing area with a similar wingspan and wing bending moment, which allows a longer endurance and a small folded size [3]. In recent research on the low-speed high lift UAV, its advantages in VSTOL, long-range cruise missiles, and tube-launch UAVs are clear [4, 5]. The supposed benefit of the tandem wing is a theoretical 50% reduction in the induced drag, but this result is not seen in practice. The tandem wing faces a fundamental problem, the rear wing must fly in the downwash of the front wing, so the direction of lift is turned. The lift of the back wing therefore has a component to the rear that is a newly created drag term [6]. That means the front and rear wings in limited space cannot avoid a dramatic wing-wing interaction impacting the aerodynamic performance, which many researches in the field of flapping wings concentrate on [7-9]. Some investigations have concluded a tandem wing with an upper front wing and a lower rear wing has significant advantages over other designs in terms of stability and aerodynamic characteristics [10], so our investigation adopts a small foldable tandem UAV design with this feature. The aerodynamic characteristic of the cross-section constructed with 2 airfoils has been well researched and optimized [11]. Based on that, some establishment and varication of the longitudinal aerodynamic model are promoted [12]. However, there are few discussions on the nonlinear pitching moment characteristic in published studies [13, 14]. In this investigation, we would figure out the reason for the pitching moment nonlinearity and try to promote some effective improvement approaches.

In the second section, an introduction of the research object which is a compact foldable tandem wing UAV is presented. after that, the design of the simulation experiment is explained in detail and a brief Computational Fluid Dynamics (CFD) method introduction follows. The third section is mainly about the discussion of the results. the simulation results of the 2 airfoils and the initial configuration are compared to distinguish the different consequences of the downwash and the complex flow in three dimensions (3D) involving the wingtip vortex and its backward rotation. Analysis of their consequences is based on conducting a comparison between the initial and lengthen configurations. The lengthening of the front wing makes the rear wing far away from the wingtip vortex, thus it can show the performance loss of the rear wing caused by downwash intensity. Two kinds of front wingtips are applied to change the wingtip vortex intensity and distribution under a strict constraint of folded size. The conclusion summarizes the flow phenomenon and its influences. Finally, the effectiveness of the pitching moment nonlinearity via modifying the front wing tip geometric is verified.

2. Methodology

2.1 Introduction to the geometry

A small tandem wing UAV is employed as the research object in our investigation, and its axonometric outline is shown in Figure 1. The UAV consists of a fuselage, two straight wings arranged in the front and rear, and 2 vertical tails on both sides. The layout that an upper front wing and a lower rear wing are selected, and both wings have a dihedral angle of 2°. The detail of the rotation mechanism at the wing root and the propulsion motor at the rear fuselage are simplified to provide a better mesh quality for CFD simulation and improve computational efficiency.

The length of the fuselage is about 1.8 m, and a customized airfoil is applied to the two wings. The front part of the fuselage is cylindrical, and some important parameters of the design are listed in Table 1. The configuration gravity center (CG) is 875mm from the fuselage's foremost point, which is used as the reference point for calculating the moment in the simulation.

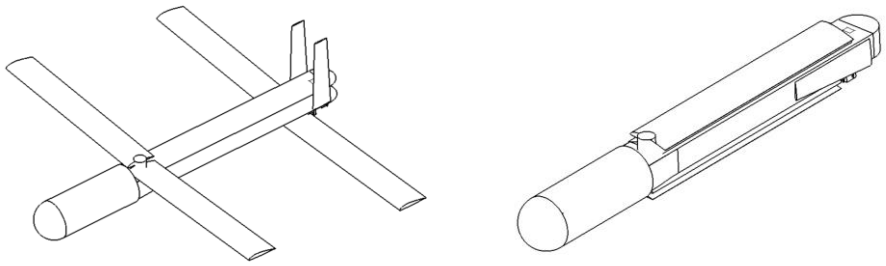

(a) (b)

Figure 1 – Axonometric view of cruise(a) and fold state(b)

Table 1 – Parameters of the configuration

Parameter Name	Value
Length	1.8 m
Height	0.45 m
Wingspan	1.875 m
Wing chord (single wing)	0.154 m
Wing area (double wing)	0.575 m^2

The total weight of the UAV is 25kg, the cruising altitude is 3km, and the cruise speed is 40m/s. The simulation atmospheric is defined by the standard atmosphere model parameters.

The left and right part of a single wing has unequal heights. They can stack up under the fuselage size after folding, which contributes to a higher folding efficiency and achieves a folded volume as small as possible. This design arranges a large wing area under the folded size constraints, which benefits the endurance and the payload capacity. For limiting the consequence of rolling and yaw moments caused by the unequal height of left and right parts, the height difference between the left and right side of the wings is designed to remain the same height. The front and rear wings with a

larger chord length can be set profit from the unequal folding height of the left and right half-wing. As a result, the ratio of the horizontal distance between the front and rear wings to the chord length of the wing becomes smaller, which means the tandem wing is more compact. the aerodynamic interference is strengthened between the front and rear wings, and the aerodynamic characteristics become worse.

2.2 Design of the simulation experiment

This investigation aims for exploring an effective method that improves the nonlinear pitching moment characteristic of the compact foldable tandem wing. Comparing the aerodynamic characteristics of the cross-section and that of 3D configuration figures out the consequences of the flow phenomenon and its generating reasons. Some close attention is paid to the front wing induced downwash and its wingtip vortex which dominates a backward rotation flow that might be the cause of the influence of aerodynamic performance. Moreover, some modification based on the UAV geometry is applied to decline the unfavorable flow phenomenon, which would be verified by the simulation.

Following this research route, we design a two-dimensional(2D) cross-section simulation consisting of 2 airfoils and 4 3D tandem wing simulations including 4 different wingtip shapes. Each simulation involves the angle of attack (AoA) ranging from -4 to 6° with 2° interval. These 3D simulations can be recognized into two categories by the wingtip shape. Figure 2(a) is the initial configuration, and the others are improved configurations (Figure 2 b/c/d). By comparing the flow phenomena and aerodynamic characteristics extracted from these CFD simulation results, we can analyze the wing-wing interaction consequences and evaluate the effectiveness of the geometric modification.

The four configurations are described briefly as follows:

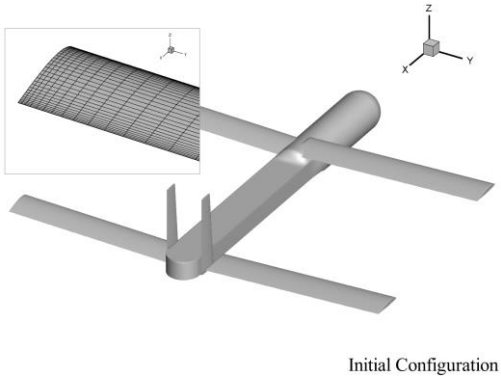

(a) Initial Configuration

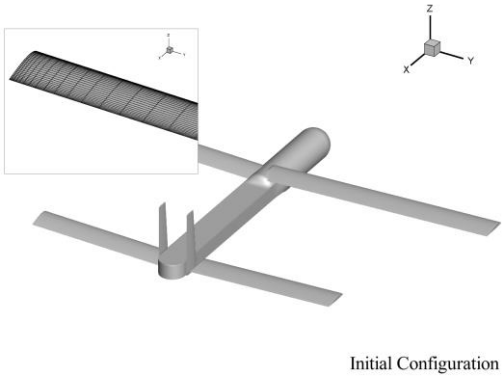

(b) Lengthen Configuration

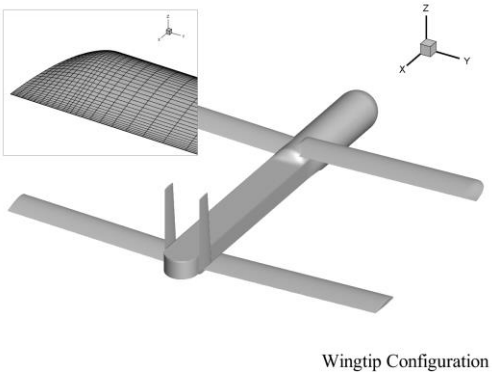

(c) Wingtip Configuration

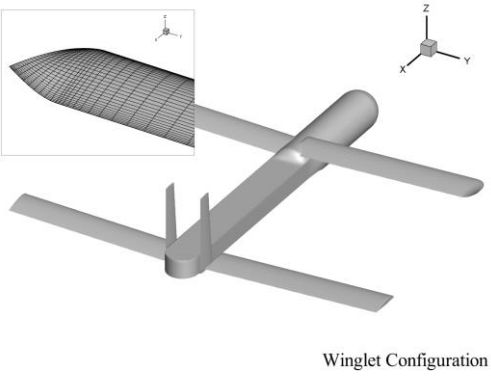

(d) Winglet Configuration

Figure 2 – Four configurations in simulation

(a) Initial configuration: The front and rear wings have the same length of chord and spanwise. The wings are flat and rectangular. Both wingtips are unmodified, i.e the airfoil shape.

(b) Lengthen configuration: The front wingspan is expanded to 1.5 times longer with the same rear wingspan. Aim to retain the same front wing downwash intensity on the rear wing and reduce the

rear wing spanwise flow intensity induced by the backward rotation flow from the front wing tip vortex.

(c) Wingtip configuration: Based on the initial configuration, a semicircular wingtip is formed by a continuous transition surface from the leading edge to the trailing edge with a straight trailing edge. The intensity of the front wing wingtip vortex is reduced and maintains the same downwash intensity as the initial configuration, which declines the influence of the wingtip vortex near the rear wing. it is a potential approach to decline the wing-wing interaction disadvantages and recover the aerodynamic efficiency of the rear wing without changing the folding size and wing area significantly.

(d) Winglet Configuration: The idea of this configuration develops from the Wingtip Configuration. A winglet that is widely used in wingtip flow control is introduced, and a slightly up-warped winglet is designed at the front wingtip. Besides weakening the intensity of the front wing wingtip vortex, its spatial position of it also can be raised. The induced influence near the rear wing surface is further reduced with an upper front wing and a lower rear wing design. The aerodynamic performance benefited from an appropriate flow control by a winglet at the tandem wing configuration can be verified apparently.

2.3 CFD method

2.3.1 Meshing method

A complete model simulation is conducted because of the configuration asymmetry, and the structure mesh is adopted to improve the mesh generation efficiency after the subsequent geometric model modification.

A cross-section at the 50% span of the tandem wing is extracted for 2D simulation. In the mesh generation process of this cross-section, the 2D structure mesh is applied. The geometric model of the tandem wing used to generate the mesh has a ratio of 1 to the real size of the UAV. The far-field size is 30 times the configuration size nearly.

Figure 3 a and b show the structure mesh of the cross-section and configuration. At the near-wall field of the geometric model, a hexahedral mesh filling the boundary layer is generated from the wall with y+=1 as the initial condition. It expands 34 layers growing outward at a rate of 1.1 to obtain a more accurate near-wall phenomenon. The amount of 2D structure mesh used for simulation is about half a million, and the amount of 3D configuration mesh is about 8 million. Utilizing the 2 × 2 × 2 structure mesh evaluation standard, all cell quality is controlled above 0.2.

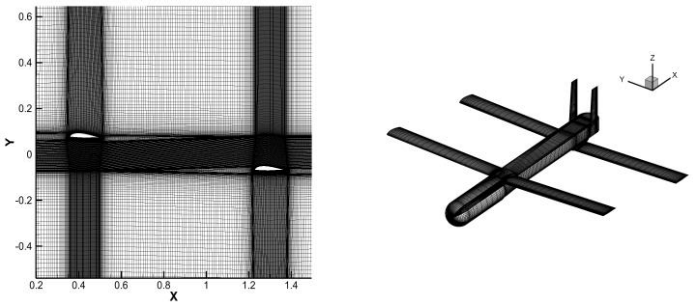

(a) (b)

Figure 3 – Mesh of the CFD simulation. (a) mesh of the cross-section, (b) mesh of the configuration

The preliminary simulations show that the structure mesh has good computational robustness and fast convergence tendency, which provides good efficiency for the research.

2.3.2 Numerical method

The Reynolds averaged Naiver-Stokes equation (RANS) is adopted. The ideal gas model is used. The k-omega turbulence model is chosen to close these equations, and the density-based implicit equations are calculated in the simulation.

The shear stress transport (SST) k-omega turbulence model is applied. The use of a k-ω formulation in the inner parts of the boundary layer makes the model directly usable all the way down to the wall through the viscous sub-layer, hence the SST k-ω model can be used as a Low-Re turbulence model without any extra damping functions. The SST formulation also switches to a k-ε behavior in the free-

stream and thereby avoids the common k-ω problem that the model is too sensitive to the inlet free-stream turbulence properties [15]. The Bradshaw hypothesis is introduced to consider the effects of Reynolds shear stress transport.

This turbulence model has good computational stability and high accuracy for the simulation in this investigation. The transport caused by turbulent shear stress can be well handled in the adverse pressure gradient and separation boundary layer, and the complex flow of that can be well predicted [16]. Therefore, the model is suitable for this flow field characteristics analysis.

3. Discussion

3.1 Comparison of the cross-sections and the initial configuration

By analyzing the results of the cross-sections and the initial configuration, the pressure coefficient (Cp) variation of the front and rear wings caused by downwash and wingtip vortex induced rotation can be revealed respectively (Figure 4 a and b). It can be concluded by the comparison of Figure 4 c and d that the downwash velocity magnitude of the 2D and 3D wing-wing flow fields is relatively close. Due to the complexity of the 3D flow, the range of that varies significantly. The magnitude of Cp decreases because of the wing-tip vortex influences on the rear wing outside surface.

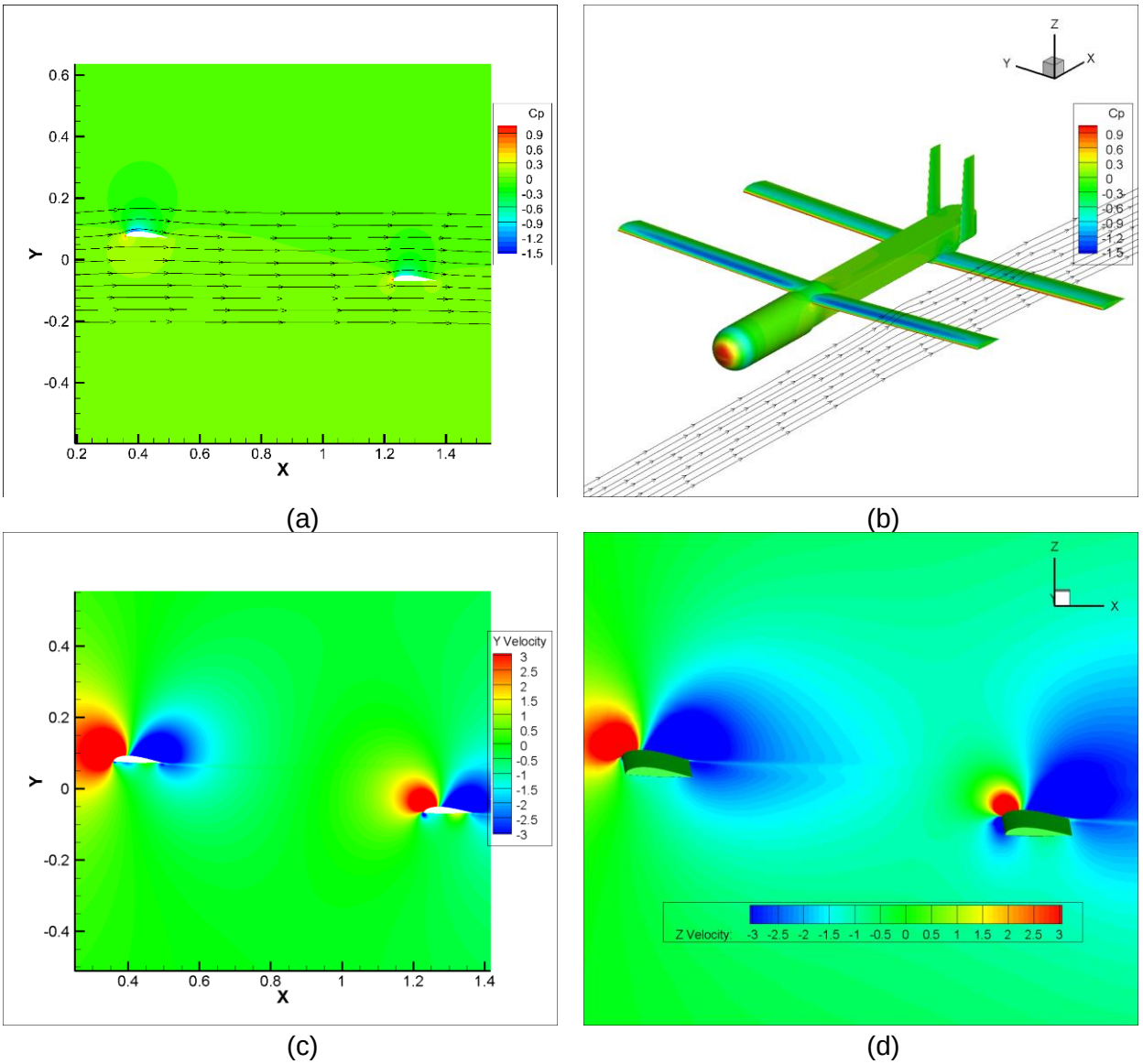

(a) (b)

(c) (d)

Figure 4 – Comparison of the 2D and 3D flow phenomenon. (a) Cp and streamline of the cross-section, (b) Cp and streamlines of the initial configuration, (c) downwash (Y-direction) velocity of the cross-section, (d) downwash (Z-direction) velocity of the slice of the configuration.

In order to explore how downwash intensity influences the rear wing aerodynamic performance. we adopt many combinations taking different front and rear wing incidence angles which accompanies the different levels of downwash intensity among the wing-wing area. Several cases are simulated, and a set of pitching characteristic curves with lift coefficient as the horizontal axis and pitching moment coefficient as the vertical axis are presented finally.

It can be demonstrated from Figure 5 that the curves shift upward with the increasing incidence angle of the front wing. all pitching characteristic curves of the cross-section that consists of 2 airfoils are relatively linear. However, a significantly nonlinear characteristic does the tandem wing configuration present. The slope differences of the curves at the negative and positive AoA can be several times, which is also shown in some tandem wing studies [13]. It should be noted that the nonlinear characteristics of the pitching moment are still consistent when the combination of front and rear wing incidence angles changes with different intensities of the inter-wing downwash. It can be concluded that the enhanced downwash by the increasing of the front wing incidence angle has a limited contribution to the nonlinear characteristics of the pitching moment.

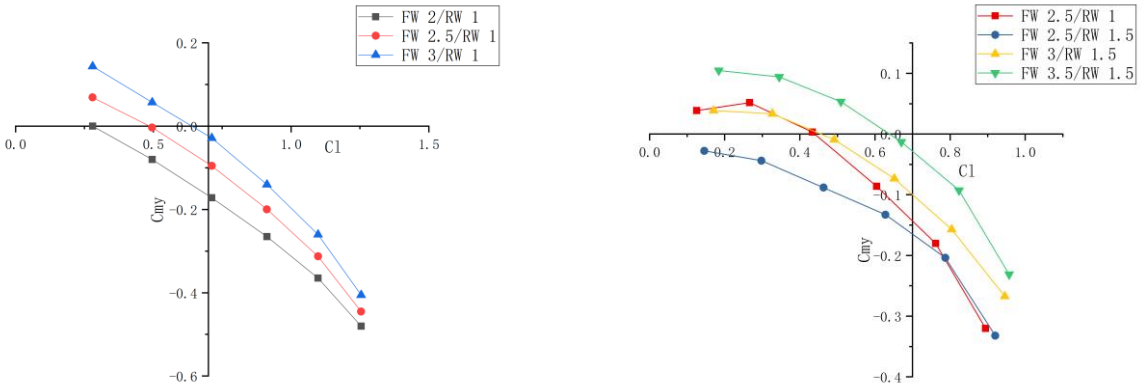

(a) (b)

Figure 5 – Comparison of the 2D and 3D aerodynamic coefficients. (a) lift to pitch moment coefficient curves with a different incidence angles of the airfoils, (b) lift to pitch moment coefficient curves with a different incidence angles of the wings.

After concluding the downwash coexisting in 2D and 3D flow fields has a limited consequence on the aerodynamic performance. It is necessary to study the backward rotation of the wingtip vortex induced by the front wing induces strong spanwise flow near the rear wing surface. From Figure 6, we can see almost 1/3 wingspan of the rear wing is affected by this backward rotation, which causes the lift loss of the rear wing outside part. The aerodynamic performance of the UAV is also significantly affected.

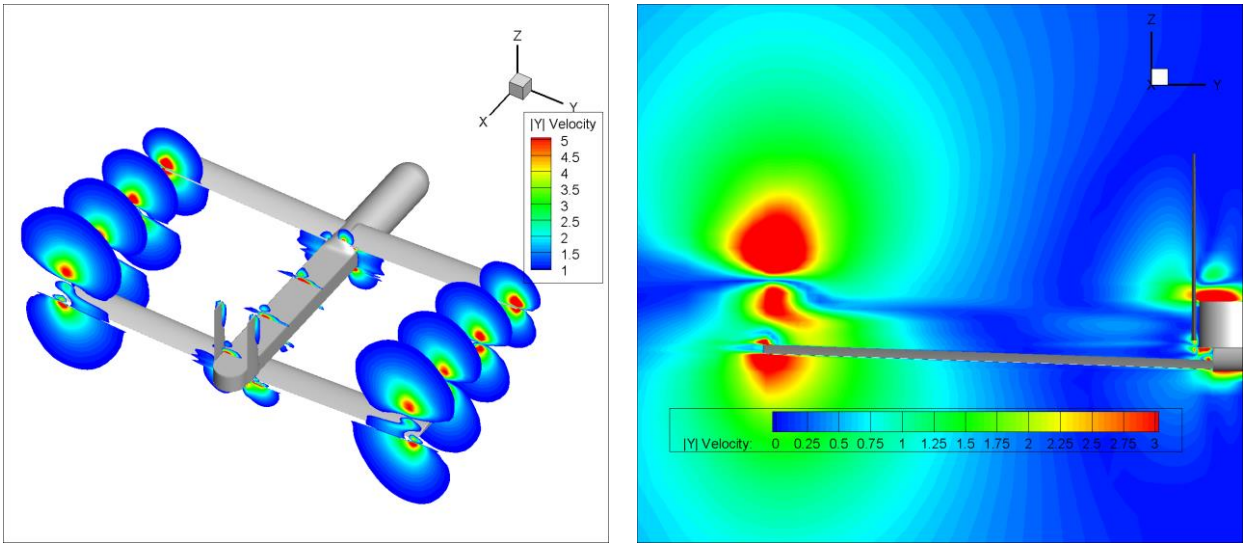

(a) (b)

Figure 6 – Analysis of the wing-wing interaction flow. (a) spanwise flow induced by the front wing, (b) slices of the spanwise velocity contour at the rear wing.

3.2 Analysis of the initial and lengthen configuration

Through the comparative analysis of the cross-section and initial configuration results, the downwash induced by the front wing to the rear wing is not the main reason for the aerodynamic performance loss of the rear wing.

The backward rotational flow induced by the front wingtip vortices leads to spanwise flow near the rear wing, which is worth exploring whether it is the cause of the nonlinearity of the pitching moment and the aerodynamic performance loss of the rear wing. To this end, the lengthen configuration is adopted in which the length of the front wing is increased by 1.5 times. In this case, the influence region of the front wing tip vortex is moved outward significantly.

The Cp contour of the configuration for the initial and lengthen configuration is shown in Figure 7:

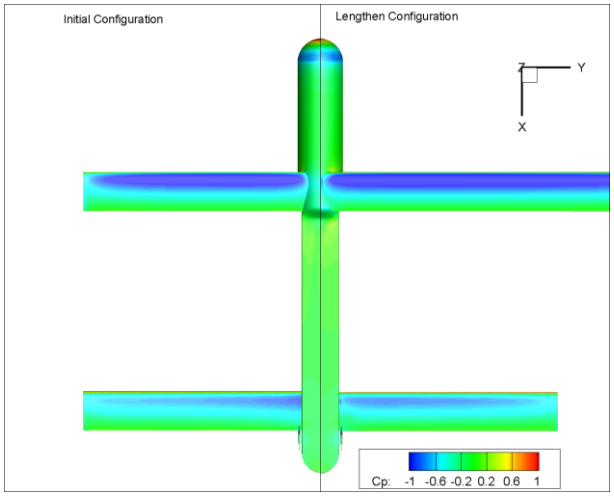

Figure 7 – Comparison of the Cp on the initial and lengthen configuration surface, the initial configuration on the left and the lengthen one on the right.

The results of the lengthen configuration show that the Y-direction velocity iso-surface induced by the front wing tip moves outward obviously (Figure 8), and the rear wingspan that is affected and the intensity of the interference are significantly reduced. The spanwise flow near the rear wing is reduced, and the effect of the tip vortex is verified.

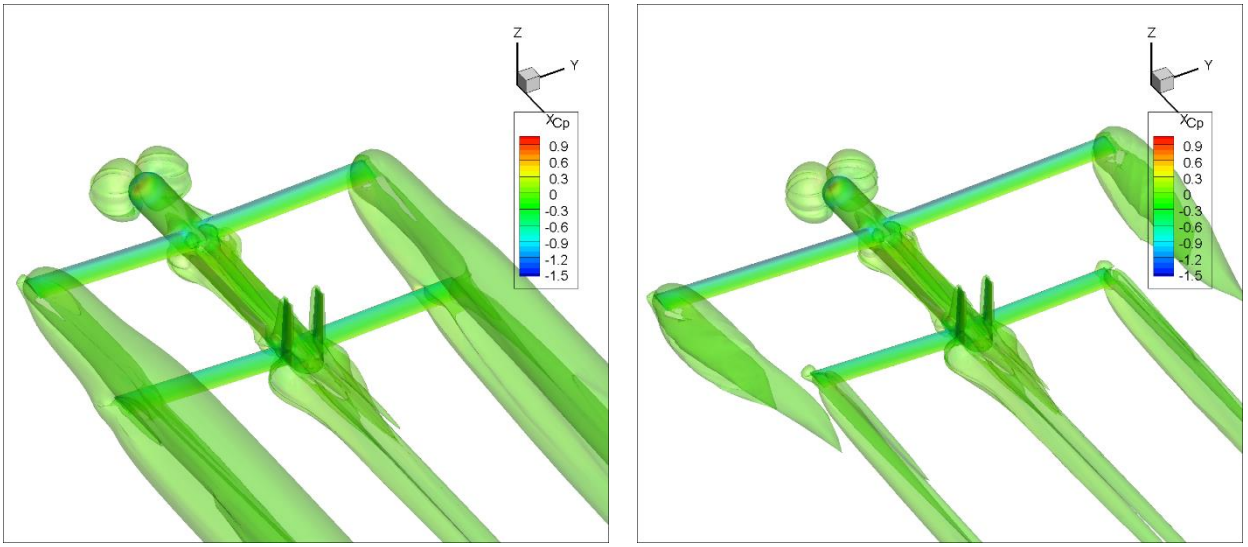

(a) (b)

Figure 8 – The iso-surface (Y velocity = 1.5m/s) induced by the front wing tip vortex. (a) initial configuration, (b) lengthen configuration.

Extracting the Cp distribution along the chordwise at different span positions of the rear wing reveals that the Cp on the upper and lower surfaces recovers (Figure 9 (a)). lengthening the front wing helps decline lift loss of the rear wing.

Extracting the Cp distribution along spanwise at the rear wing 1/4 chord length reveals that the weaker interference intensity from the front wing tip vortex reduces the negative pressure on the rear wing upper surface and increases the negative pressure on its lower surface, which increases the lift of the rear wing (Figure 9 (b)).

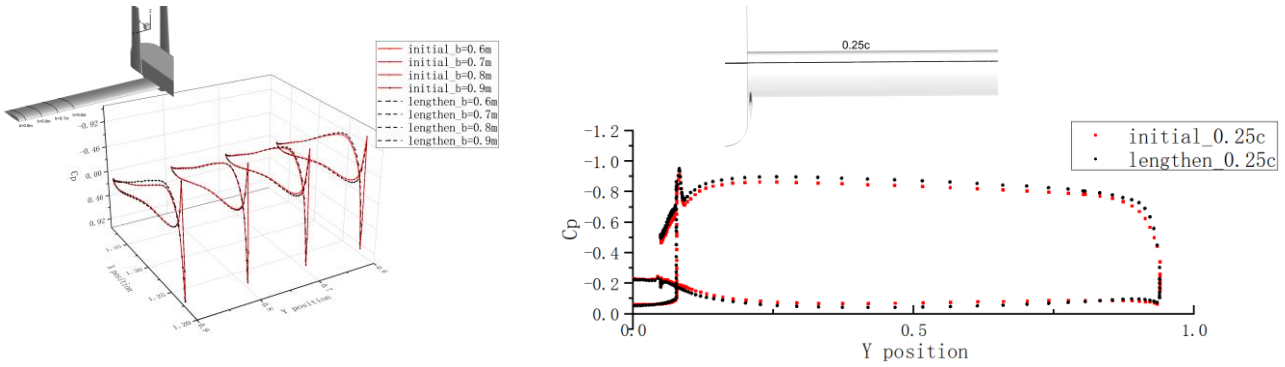

(a) (b)

Figure 9 – Comparison of the Cp distribution between the initial configuration and lengthen configuration. (a) at 0.7/0.8/0.9/1 wingspan ratio, (b)at the 0.25 chord ratio.

Comparing the pitching moment characteristics of the initial and lengthen configuration is not suitable to explain the improvement because the lengthened front wing span changes the wing area making the configuration trim change. However, it can be proved that the rear wing lift to drag ratio is improved and the drag is reduced, which is benefited by a weakened spanwise flow intensity near the rear wing (Figure 10 a/b). The aerodynamic center moves backward which can provide a more linear pitch moment characteristic.

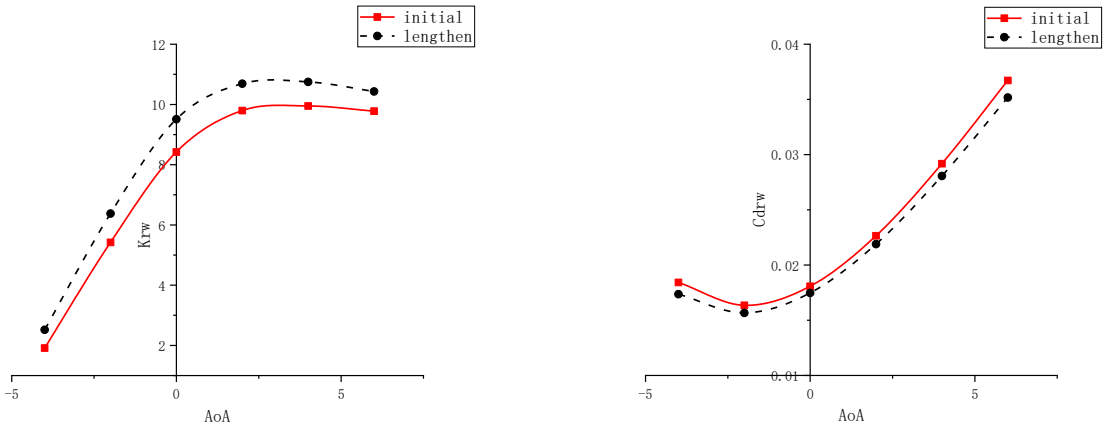

(a) (b)

Figure 10 – Comparison of the initial and lengthen configuration aerodynamic coefficient. (a) lift-to-drag ratio of the rear wing, (b) drag coefficient of the rear wing.

3.3 Analysis of the wingtip and winglet configuration

The results comparison between the lengthen configuration and the initial configuration verifies that weakening the influence of the front wing tip vortex on the rear wing can improve the pitching moment characteristics effectively. However, the compact foldable tandem wing has strict size restrictions after being folded in most cases, and it is necessary to realize the effective recovery of the rear wing aerodynamic efficiency on the premise of changing the initial configuration as small as possible. Therefore, two kinds of wingtip modification geometry, the wingtip and winglet configuration, are studied.

The comparison of the Cp of the two modifications compared with the initial layout shows that the two wingtip shapes achieve an improvement of the influence effect, and the rear wing Cp on its surface has recovered as can be seen in Figure 11 a and b.

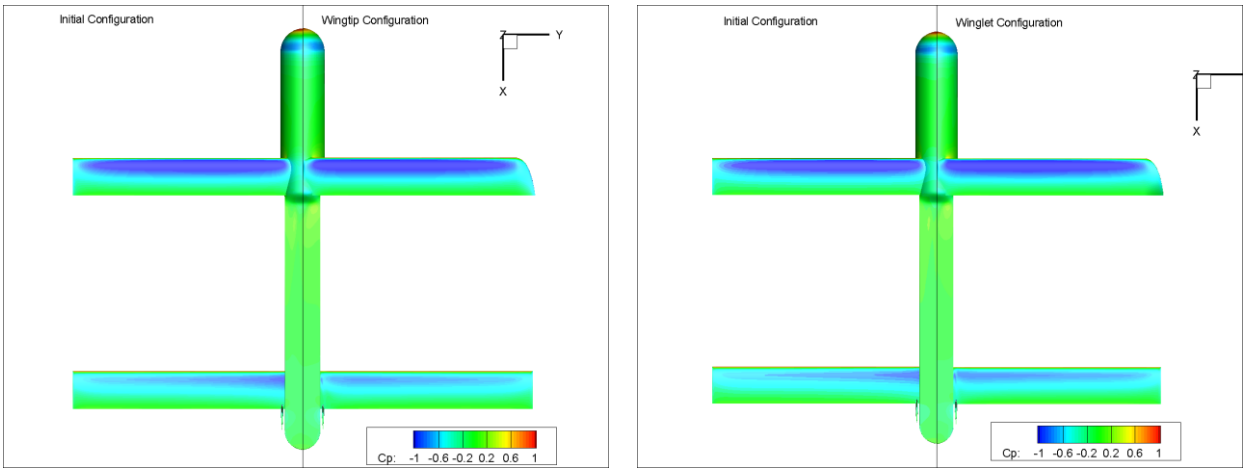

(a) (b)

Figure 11 – Comparison of the Cp on the surface. (a) initial configuration on the left and wingtip configuration on right, (b) initial configuration on left and winglet configuration on right.

From the Y direction velocity iso-surface induced by the front wingtip (Figure 12 a and b), it demonstrates that the wingtip configuration has an influence on the strength of the wingtip vortex, which reduces the affected rear wings span compared with the initial configuration relatively. Compare with the wingtip, the winglet configuration weakens the strength of the wingtip vortex further and adjusts the influenced field of the wingtip vortex upwards simultaneously. It presents that the area where the Cp of the rear wing surface decays is smaller, and the value decreases less at the same AoA.

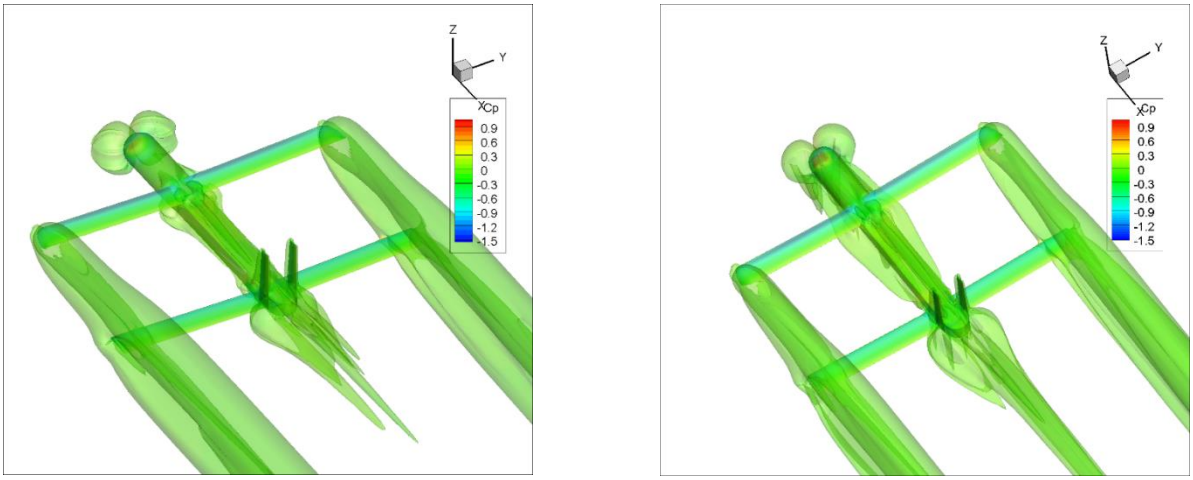

(a) (b)

Figure 12 – The iso-surface (Y-velocity = 1.5m/s) induced by the front wing tip vortex. (a) wingtip configuration, (b) winglet configuration.

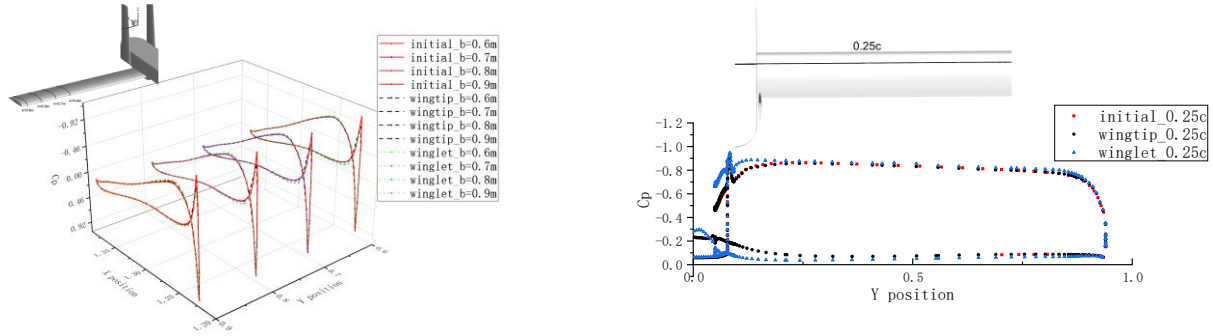

(a) (b)

Figure 13 – Comparison of the Cp distribution between the initial configuration, wingtip configuration, and winglet configuration. (a) at 0.7/0.8/0.9/1 wingspan ratio, (b)at the 0.25 chord ratio.

By extracting the Cp distribution along the chordwise at different span positions and 1/4 chord positions of the wingtip and winglet configuration and comparing them with the initial ones (Figure 13 a and b). It can be concluded that the winglet configuration has a better recovery of the Cp at the rear wing surface than the wingtip configuration. Both geometry modifications have the aerodynamic performance improvement. The Cp distribution on the upper and lower surfaces of the rear wing is disturbed more slightly, which could promote the linearity of the pitching moment characteristics and the aerodynamic performance (Figure 14 a and b).

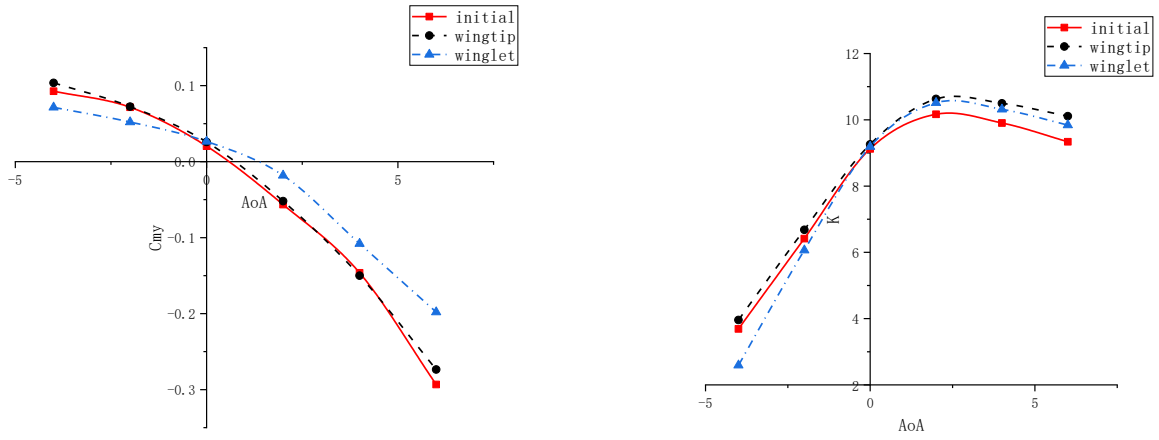

(a) (b)

Figure 14 – Comparison of the initial, wingtip, and winglet configuration aerodynamic coefficient. (a) the pitching moment coefficient of the configuration, (b) lift-to-drag ratio of the configuration.

4. Conclusion

In this investigation, the analysis of the flow phenomenon and aerodynamic characteristics between the 2D cross-section and 3D tandem wing configuration simulation shows that the downwash caused by the front wing is not a significant factor in the pitching moment nonlinearity. However, the backward rotation flow induced by the front wing tip is the main reason, which governs the spanwise flow near the rear wing. As the AoA decreases, the longitudinal distance between the front and rear wing decreases with an increasing affected span of the rear wing in the backward rotation flow field from the front wingtip. it is the mechanism why a remarkable rear wing aerodynamic efficiency decreases on tandem wing configuration happened, which contributes to a forward center of aerodynamic tendency decreasing the slope of the pitching moment curve.

By comparing the simulation results of the initial with the lengthen configuration that has 1.5 times lengthened front wingspan. It realizes that the downwash effect of the front wing is preserved while the influence of the front wing tip vortex on the surface flow of the rear wing is reduced. The aerodynamic efficiency and the lift-drag ratio of the rear wing improve. Adjusting the strength and position of the wingtip vortex is a feasible approach to improve the pitching moment nonlinear characteristics of the configuration.

In order to satisfy the size constraints of the compact foldable tandem wing configuration well, it is necessary to find a reasonable geometry modification for weakening the intensity and adjusting the position of the front wing tip vortex. The results show both the wingtip and winglet configuration can achieve an aerodynamic characteristics improvement. Generally, the effect of the winglet configuration is better than the wingtip one. A reasonably modified shape of the front wing tip does improve the performance of the rear wing, which declines the aerodynamic center forward tendency. It is effective to improve the pitching moment characteristics and configuration aerodynamic performance.

Future work could concentrate on the parametric optimization method of the winglet shape for tandem wing configuration, which has to be under the constraint of the folded size and the aerodynamic efficiency. Moreover, the results of the cross-section with 2 airfoils are not accurate in revealing the aerodynamic characteristics of the configuration, especially the nonlinear longitudinal aerodynamic characteristics. Through parametric modeling and machine learning, it is the potential to achieve a prediction method of the tandem wing aerodynamic characteristics based on some effective data of its cross-section analysis.

5. Contact Author Email Address

Mail to: wangxiangsheng@buaa.edu.cn

6. Copyright Statement

References

[1] Hardin PJ, Jensen RR. Small-scale unmanned aerial vehicles in environmental remote sensing: Challenges and opportunities. *GISCI REMOTE SENS* 2011;48(1):99-111.

[2] Selitrennik E, Karpel M, Levy Y. Computational aeroelastic simulation of rapidly morphing air vehicles. *J AIRCRAFT* 2012;49(6):1675-86.

[3] Guangjia L, Feng L, Wen S. Numerical Simulation of Tandem-airfoil. *AIRCRAFT DESIGN* 2006. 2006-03-30(01):19-24.

[4] Tomasz G, Marcin F. Aerodynamic and stability analysis of personal vehicle in tandem-wing configuration. *Proceedings of the Institution of Mechanical Engineers, Part G: Journal of Aerospace Engineering* 2017. 2017-09-15;231(11).

[5] Yongze S, Chuanjie S, Yonggang L. Studying the Impact of Aerodynamic Characteristics Due to the Relative Position of the Wing for the Tandem Wing. *AIRCRAFT DESIGN* 2016.2016-12-15;36(06):32-6.

[6] Raymer D. *Aircraft design: a conceptual approach*: American Institute of Aeronautics and Astronautics, Inc.; 2012.

[7] Peng L, Zheng M, Pan T, Su G, Li Q. Tandem-wing interactions on aerodynamic performance inspired by dragonfly hovering. *ROY SOC OPEN SCI* 2021;8.

[8] Broering T, Lian Y. *The Effect of Wing Spacing on Tandem Wing Aerodynamics*.

[9] Zhang GQ, Yu SCM. Unsteady Aerodynamics of a Morphing Tandem-Wing Unmanned Aerial Vehicle. *J AIRCRAFT* 2012;49(5):1315-23.

[10]Cheng H, Wang H, Menglong W, Qingli S. Comparison of layout scheme for the tandem wing loitering aerial vehicles with different aerodynamic configurations and control surfaces. *FLIGHT DYNAMICS* 2019 2018-11-07;37(01):28-33.

[11]Yunhao W, Wenwu Z, Xinzhe Z, Jun D. Numerical analysis of two-dimensional tandem-airfoil. *JOURNAL OF CHANGCHUN UNIVERSITY OF TECHNOLOGY* 2021 2021-06-15;42(03):259-66.

[12]Wang Z, Xiong J, Cheng X, Li J. Establishment and verification of longitudinal aerodynamic model of tandem wing aircraft. IOP conference series. *Materials Science and Engineering* 2019 2019-01-01;563(3):32022.

[13]Jinchao M, Chunyuan Z, Xiang L, Anming C. Study on Effect of Propeller Distribution on Aerodynamic Characteristics of Small Tandem-Wing UAV. *Journal of Ordnance Equipment Engineering* 2020 2019-12-27;41(05):54-9.

[14]Gao L, Jin H, Zhao J, Cai H, Zhu Y. Flight dynamics modeling and control of a novel catapult launched tandem-wing micro aerial vehicle with variable sweep. *IEEE ACCESS* 2018;6:42294-308.

[15]Könözsy L. *A new hypothesis on the anisotropic Reynolds stress tensor for turbulent flows*: Springer; 2019.

[16]Menter F. Zonal two equation kw turbulence models for aerodynamic flows. *23rd fluid dynamics, plasmadynamics, and lasers conference*; 1993; 1993. p. 2906.